Electronic Supplementary Material (ESI) for Physical Chemistry Chemical Physics.

Supporting Information

A first-principles study of electro-catalytic reduction of CO_2 on Transition Metal Doped Stanene

Sudatta Giri[1], Satyesh K Yadav[2], Debolina Misra[1,*]

[1]Materials Modelling and Simulation Laboratory, Department of Physics, Indian Institute of Information Technology, Design and Manufacturing, Kancheepuram, Chennai, India, 600127.

[2]Department of Metallurgical and Materials Engineering, Indian Institute of Technology Madras, India, 600036.

Corresponding author: debolinam@iiitdm.ac.in

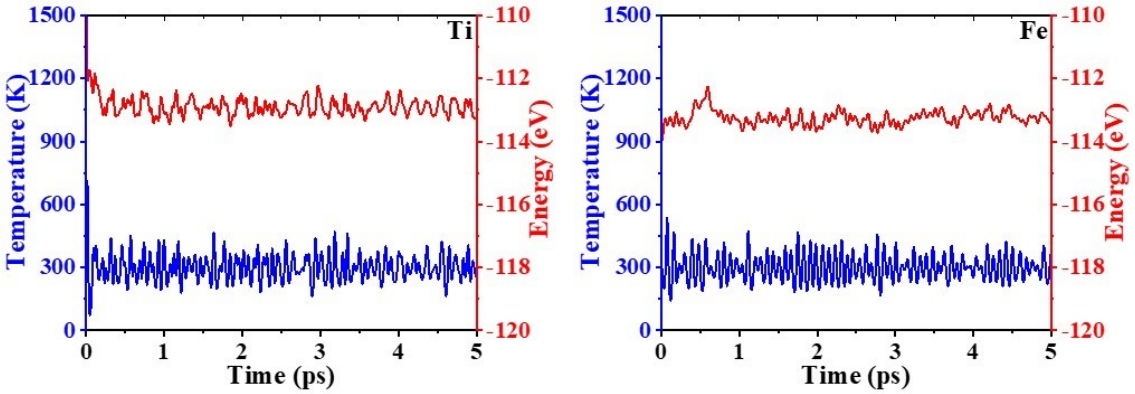

Figure S1: Energy and temperature variation for Ti- and Fe- doped stanene at 300 K for 5 ps.

Adsorbate	ZPE (eV)	-TS (eV)	G – E_{elec} (eV)
$^*CO_2$	0.330	-0.255	0.075
$^*COOH$	0.619	-0.098	0.521
$^*CO$	0.219	-0.131	0.088
$^*OCHO$	0.592	-0.158	0.434
$^*HCOOH$	0.940	-0.150	0.790

Table S1: Contributions of zero-point energy and entropic corrections[1,2] to adsorbate free energies

Electro-chemical stability:

Energy of formation of pure and TM-doped stanene are calculated as[3]

$\Delta E = E(Sn_xM_y) - xE_{sn} - yE_M$

Here M denotes the TM SA, x and y are the numbers of Sn and TM atoms respectively. ΔE for pure stanene is calculated to be -0.258 eV/Å^2. For TM@Sn, ΔE values are listed in Table S2.

The dissolution potential for TM@Sn is calculated as [4],

$$U_{Diss} = U_{Diss}^{0} - \frac{E_{TM-Sn} - E_{Sn} - \mu_m}{ne}$$

Where U_{Diss}^{0}, n and e are standard dissolution potential of metal, number of electron involved in dissolution and electronic charge respectively and the corresponding values of U_{Diss}^{0} and n are taken from existing literature[4]. E_{TM-Sn} and E_{Sn} are the energies of stanene layer with and without TM atom, μ_m is the chemical potential of the TM SA with gaseous energy reference representing implantation of TM SA as reported previously in similar hosts [5–11].

The dissolution potentials for TM@Sn (TM: Ti, Fe) are listed below in Table S2.

TM	ΔE **(eV/Å²)**	U_{Diss}^{0} **(V)**	**n**	μ_m**(eV)**	U_{Diss}^{G}**(V)**
Ti	-0.271	-1.63	2	-2.332	0.53
Fe	-0.268	-0.45	2	-3.236	1.12

Table S2: Energy of formation/area and Dissolution potentials for TM@Sn.

With crystalline energy reference for the TM SAs, the energy of formation for Ti@Sn and Fe@Sn are 1.08 eV and 1.75 eV respectively. Both these values are significantly lower than the formation energies reported for similar 2D materials such as free-standing or graphene with single and double vacancies [12,13], within the same level of theory. The values however will change if improved DFT functional such as DFT+U [4] or hybrid functional [3] HSE06 is adopted.

Hydrogen Bond Strength:

The possibility of H-bond formation between the activated CO_2 and the nearby H_2O molecules is realized through the interaction energies (E_{in}) between these two molecules, calculated as per the super-molecular approach[12],

$$E_{in} = E_{AB} - E_A - E_B$$

Where E_A, E_B, and E_{AB} are the energies of the optimized CO_2, H_2O molecules and of the complex formed due to their co-adsorption respectively [14]. Our calculated E_{in} values are -0.08 eV and -0.07 eV for Ti and Fe-doped stanene respectively, indicating that formation of H-bond is favourable.

For Ti@Sn and Fe@Sn, the distances between (i) oxygen atoms of H_2O and CO_2 are 2.837 Å and 2.905 Å, and (ii) oxygen atom of H_2O and carbon atom of CO_2 are 4.06 Å and 4 Å respectively, both shorter than 4.19 Å, the sum of Van der walls radii of Carbon (1.7 Å), Oxygen (1.52 Å) and O-H bond length in H_2O (0.97 Å).

The bader charges on the oxygen atom of H_2O (charge accumulation) and carbon atom of CO_2 (charge depletion) for both the catalysts are listed below in Table S3.

Catalysts	**Bader charge q (e)**	
	q_C^{CO2}	q_O^{H2O}
Ti@Sn	+1.15	-1.27
Fe@Sn	+1.47	-1.37

Table S3: Bader charge analysis for C atom in CO_2 and O atom in H_2O.

References:

1 S. Zhou, W. Pei, J. Zhao and A. Du, Silicene catalysts for CO_2 hydrogenation: the number of layers controls selectivity, *Nanoscale*, 2019, **11**, 7734–7743.

2 Y. Yang, J. Li, C. Zhang, Z. Yang, P. Sun, S. Liu and Q. Cao, Theoretical Insights into Nitrogen-Doped Graphene-Supported Fe, Co, and Ni as Single-Atom Catalysts for CO_2 Reduction Reaction, *J. Phys. Chem. C*, 2022, **126**, 4338–4346.

3 X. Li, H. Li, X. Zuo, L. Kang, D. Li, B. Cui and D. Liu, Chemically Functionalized Pentastanene Monolayers for Light Harvesting with High Carrier Mobility, *J. Phys. Chem. C*, 2018, **122**, 21763–21769.

4 L. Gong, X. Wang, T. Zheng, J. Liu, J. Wang, Y.-C. Yang, J. Zhang, X. Han, L. Zhang and Z. Xia, Catalytic mechanism and design principle of coordinately unsaturated single metal atom-doped covalent triazine frameworks with high activity and selectivity for CO_2 electroreduction, *J. Mater. Chem. A*, 2021, **9**, 3555–3566.

5 P.-C. Lin, R. Villarreal, S. Achilli, H. Bana, M. N. Nair, A. Tejeda, K. Verguts, S. De Gendt, M. Auge, H. Hofsäss, S. De Feyter, G. Di Santo, L. Petaccia, S. Brems, G. Fratesi and L. M. C. Pereira, Doping Graphene with Substitutional Mn, *ACS Nano*, 2021, **15**, 5449–5458.

6 Y. Dong, Y. Deng, J. Zeng, H. Song and S. Liao, A high-performance composite ORR catalyst based on the synergy between binary transition metal nitride and nitrogen-doped reduced graphene oxide, *J. Mater. Chem. A*, 2017, **5**, 5829–5837.

7 L. Yan, H. Jiang, Y. Xing, Y. Wang, D. Liu, X. Gu, P. Dai, L. Li and X. Zhao, Nickel metal–organic framework implanted on graphene and incubated to be ultrasmall nickel phosphide nanocrystals acts as a highly efficient water splitting electrocatalyst, *J. Mater. Chem. A*, 2018, **6**, 1682–1691.

8 F. Ren, M. Yao, M. Li and H. Wang, Tailoring the Structural and Electronic Properties of Graphene through Ion Implantation, *Materials*, 2021, **14**, 5080.

9 L. Baraton, Z. He, C. S. Lee, J.-L. Maurice, C. S. Cojocaru, A.-F. Gourgues-Lorenzon, Y. H. Lee and D. Pribat, Synthesis of few-layered graphene by ion implantation of carbon in nickel thin films, *Nanotechnology*, 2011, **22**, 085601.

10 D. Misra and S. K. Yadav, Prediction of Site Preference of Implanted Transition Metal Dopants in Rock-salt Oxides, *Sci Rep*, 2019, **9**, 12593.

11 D. Misra and S. K. Yadav, Nb-Implanted BaO as a Support for Gold Single Atoms, *J. Phys. Chem. C*, 2021, **125**, 28059–28066.

12 L. Wang, X. Zhang, H. L. W. Chan, F. Yan and F. Ding, Formation and Healing of Vacancies in Graphene Chemical Vapor Deposition (CVD) Growth, *J. Am. Chem. Soc.*, 2013, **135**, 4476–4482.

13 A. A. El-Barbary, R. H. Telling, C. P. Ewels, M. I. Heggie and P. R. Briddon, Structure and energetics of the vacancy in graphite, *Phys. Rev. B*, 2003, **68**, 144107.

14 L. Bondesson, K. V. Mikkelsen, Y. Luo, P. Garberg and H. Ågren, Density functional theory calculations of hydrogen bonding energies of drug molecules, *Journal of Molecular Structure: THEOCHEM*, 2006, **776**, 61–68.